Environ Earth Sci (2015) 73:581–592
DOI 10.1007/s12665-014-3173-1

THEMATIC ISSUE

The effect of subarctic conditions on water resources: initial results and limitations of the SWAT model applied to the Kharaa River Basin in Northern Mongolia

Lisa Hülsmann · Tobias Geyer · Christian Schweitzer · Jörg Priess · Daniel Karthe

Received: 27 June 2013 / Accepted: 20 February 2014 / Published online: 14 June 2014
© Springer-Verlag Berlin Heidelberg 2014

Abstract In Northern Mongolia, water resources are stressed by an increasing water demand for water supply in households, agriculture and mining as well as by climate and land-use changes. This study aims to obtain a better understanding of the complex hydrological processes in the semiarid, subarctic Kharaa River Basin (KRB). Therefore, the water balance components and the characteristic patterns of the river hydrograph were systematically analyzed to identify the stream flow generating processes in the catchment. The distributed, physically-based Soil and Water Assessment Tool (SWAT) model was employed for simulation of stream flow under the particular hydrological conditions. During the period 1991–2002, roughly 87 % of precipitation ($P = 216$–417 mm/year) was lost due to evaporation, leaving only a small portion of water available for stream flow and groundwater recharge. The Kharaa's hydrograph shows striking recurring patterns. River runoff in summer occurs as a response to strong summer rainfall events while stream flow generation in spring is almost exclusively driven by the melt of snow and river icings. This results in an inter-seasonal redistribution of water resources being effective for stream discharge in spring rather than in winter. Due to frozen soils, stream flow in spring is mainly generated by surface runoff and interflow. The thawing of the active layer during summer allows increased groundwater recharge. Stream flow during winter is reduced by continuously forming aufeis. Our results show that SWAT satisfactorily reflects stream flow for single years but is not reliable for a longer time period. Melt water from snow and icings could not be sufficiently simulated. The analysis reveals that refinements of SWAT are required, e.g. coupling a river ice model in order to deal with the subarctic situation in the KRB.

Keywords Mongolia · Subarctic · Aufeis · Permafrost · SWAT

Electronic supplementary material The online version of this article (doi:10.1007/s12665-014-3173-1) contains supplementary material, which is available to authorized users.

L. Hülsmann (✉)
Research Unit Forest Resources and Management, WSL Swiss Federal Institute for Forest, Snow and Landscape Research, Zürcherstrasse 111, 8903 Birmensdorf, Switzerland
e-mail: lisa.huelsmann@wsl.ch

L. Hülsmann · T. Geyer
Department Applied Geology, Geoscience Centre, University of Göttingen, Goldschmidtstrasse 3, 37077 Göttingen, Germany

C. Schweitzer · J. Priess
Department Computational Landscape Ecology, Helmholtz-Center for Environmental Research UFZ, Permoserstraße 15, 04318 Leipzig, Germany

D. Karthe
Department Aquatic Ecosystems Analysis and Management, Helmholtz-Center for Environmental Research UFZ, Brückstrasse 3a, 39114 Magdeburg, Germany

Introduction

In the catchment of the Kharaa River in Northern Mongolia, water resources are stressed by an increasing water demand for drinking water supply, agriculture and mining due to vast socio-economic changes. At the same time, the area faces climate and land-use changes. Focusing on the development and implementation of sustainable Integrated Water Resource Management (IWRM) strategies, a detailed understanding and prediction of the water balance components and the particular hydrological processes are necessary.

The hydrology of the Kharaa River Basin (KRB) is characterized by semiarid, subarctic conditions. Only a small portion of precipitation is available for infiltration and surface runoff due to large evapotranspiration losses ranging between 80 and 90 % of precipitation (MoMo-Consortium 2009). In addition, the subarctic climate fundamentally modifies the flow paths for water and its availability for evaporation and runoff by freezing and thawing of surface and subsurface water (Woo et al. 2000). Common subarctic phenomena in the catchment are snow, permafrost and aufeis (Grayson 2010). Especially, the latter two are characteristics of extreme climates, which considerably hamper the application of common hydrological models and an appropriate management of water resources.

Where the subsurface temperature remains below 0 °C continuously for 2 or more years, permafrost occurs (Sloan and Van Everdingen 1988). According to Bolton (2006), who modeled hydrological processes in areas of discontinuous permafrost, none of the common hydrological models 'is suited to handle the rapidly changing thermal (permafrost versus non-permafrost and active layer development) and hydraulic (hydraulic conductivity and storage capacity) conditions' of subarctic hydrological regimes. Hence, modifications in terms of spatially and temporally varying thermal and hydraulic soil properties are required to account for subarctic conditions.

The Kharaa River and its tributaries are covered by aufeis fields during several months, which are formed by freezing of water that continuously seeps from the ground (Williams 1970). Melting of this above-ground storage of groundwater causes an inter-seasonal redistribution of water resources from winter to spring (Sloan and Van Everdingen 1988) that needs to be considered in hydrological modeling. River ice formation and break-up processes are generally not included in hydrological models but are simulated with specialized kinematic models (Beckers et al. 2009). Although icings are common for arctic and subarctic rivers, their creation is still not fully understood (Hu and Pollard 1997), which complicates the incorporation into models.

The KRB was chosen as a case study area for the development of an IWRM project because it represents the physical and socio-economic conditions in Northern Mongolia and other regions in Central Asia. Several studies on various aspects of an IWRM were conducted within the framework of the project 'IWRM-MoMo' improving the knowledge on water- and land-related topics (Hofmann et al. 2010, 2014; Karthe et al. 2013, 2014; Menzel et al. 2011; MoMo-Consortium 2009; Priess et al. 2014). However, a comprehensive analysis of subarctic phenomena and an appropriate representation of stream flow generating processes in hydrological modeling were previously not carried out.

This study aims to obtain a better understanding of the complex hydrological processes and intra-annual dynamics in the semiarid, subarctic KRB. Therefore, the water balance components and the characteristic patterns of the river hydrograph were systematically analyzed to identify the stream flow generating processes. The distributed, physically-based Soil and Water Assessment Tool model (SWAT) (Arnold et al. 1998) was employed for the simulation of stream flow using spatial datasets on soil, land-use, climate and stream network. The SWAT model was selected since it is one of the most commonly used and well-supported hydrological models being able to assess the impact of varying land management practices on water resources and pollution. The model is applicable on medium to large scale basins with changing socio-economic and bio-physical conditions (Arnold et al. 1998). Emphasis was laid on the effects of snow, permafrost and river icings and the suitability and limitations of SWAT in simulating these processes. Developing a robust SWAT model applicable under semiarid and subarctic conditions may provide an effective tool to analyze IWRM options and scenarios in the KRB dealing with the impacts of global climate change, sectoral water use, diffuse pollution, mining and waste water inflow from rural and urban areas.

Materials and methods

Study catchment

The Kharaa River is located in Northern Mongolia between the latitudes 47°53′ and 49°38′N and the longitudes 105°19′ and 107°22′E and belongs to the Selenga–Baikal Basin. Approximately 133,000 people live within the KRB, which covers an area of 14,500 km^2 (MoMo-Consortium 2009). The altitude is 1,167 m above sea level on average. Maximum altitudes up to 2,668 m are reached in the Khentii Mountains, which are located in the eastern part of the catchment (Fig. 1). The latter is characterized by mid to high mountain ranges with steep slopes. Broader valleys, gentle hills and peneplains are found in the middle and lower parts of the basin.

The climate of the KRB can be assigned to the dry Köppen Climate Classes 'Dwc' (boreal climate with cold and very dry winters) and 'BSk' (cold, semiarid steppe climate) (MoMo-Consortium 2009). Mean annual air temperature varies between −3.7 °C in the mountains and 0.6 °C in the lower regions. During the short summers, mean monthly air temperature reaches more than 15 °C in June. Winters are cold and long with a mean monthly air temperature of −25 to −20 °C in January. Observations in the last decades reveal that air temperatures are increasing in the KRB. In Mongolia, air temperatures have increased

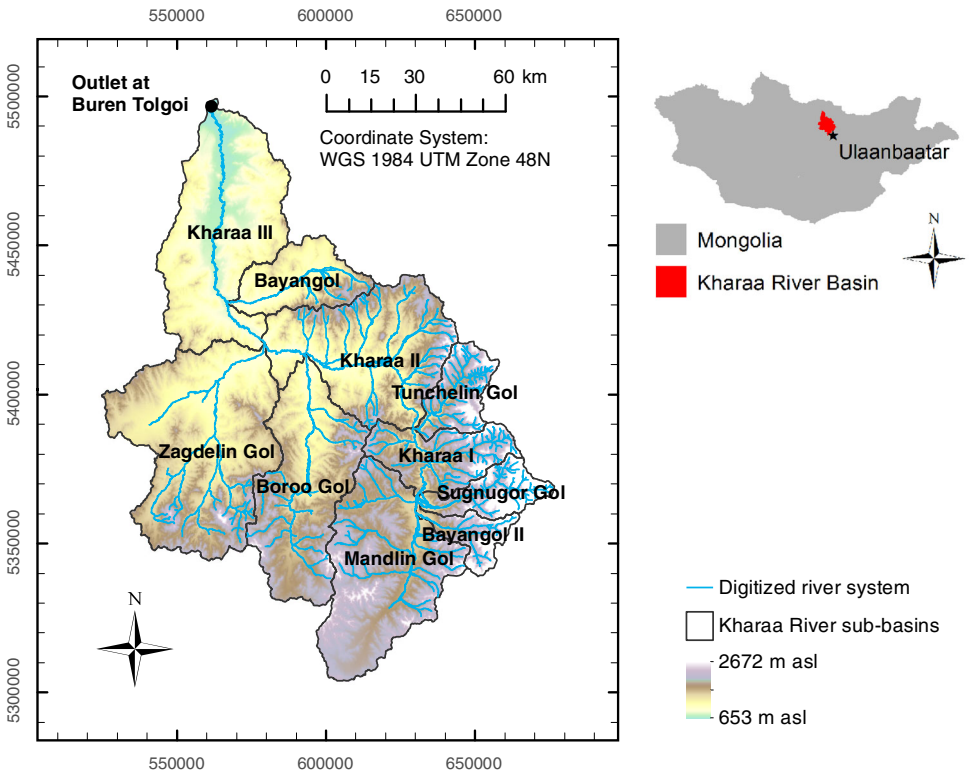

Fig. 1 Elevation, river network and sub-basins of the Kharaa River Basin

on average by 2 °C in the last 70 years (Batimaa et al. 2011). Precipitation in the investigated catchment is comparatively low and has a large spatial and temporal variability. Annual precipitation increases with elevation from 260 mm in the center of the study region to more than 400 mm in the eastern mountain range. Only 20 % of the annual precipitation occurs in wintertime, which results in a thin snow cover of 0.5–25 cm (Batima et al. 2005). Snow is reduced by intense sublimation that causes losses up to 80 % of snow water equivalent (Wimmer et al. 2009).

The Kharaa with a length of 362 km flows from the south-eastern headwaters to the north-western outlet, where it discharges into the Orkhon River (MoMo-Consortium 2009). In some areas along the Kharaa River and its major tributaries, extensive marshes and floodplains are formed due to inundation in spring and summer. Discharge at Buren Tolgoi was 12.1 m^3/s in the period of 1990–2008. As a consequence of high evaporation losses, the specific runoff of 0.83 $L/s/km^2$ is comparatively low. The main part of runoff is generated in the eastern headwater regions located in the Khentii Mountains (see Fig. 1; e.g., Sugnugur Gol, Bayan Gol II).

Since grassland covers large parts of the catchment, mainly soil types of continental dry grasslands such as Kastanozems were formed (Iderjavkhlan 2008; MoMo-Consortium 2009). In the mountainous and forested parts of the catchment, which are typically characterized by lower air temperature and higher precipitation, Umbrisols and Phaeozems are the dominant soil types. At the steep slopes along the valleys of the Kharaa River, very shallow Leptosols over continuous rock exist, while the river itself is surrounded by Fluvisol, a typical soil type in alluvial deposits (Tab S1, for a soil map of the KRB refer to Priess et al. 2014 in the same issue). The extent and productivity of aquifers in the catchment are heterogeneous. In the mountainous areas, bedrocks with local, limited aquifers prevail (Mun et al. 2008). Aquifers are also restricted in zones with the presence of loam, hard rock plates and in steep and rocky mountain slopes as well as in permafrost areas. Along the rivers, the aquifers are more productive due to unconsolidated sediments that accumulated during the Quaternary in the river valleys (Menzel et al. 2011). The sediments form an aquifer that reaches a depth of 70 m with a width of 10–20 km in the Kharaa Valley near the city of Darkhan, located in the northern part (MoMo-Consortium 2009).

Permafrost in the investigated area is continuous above 1,400–2,000 m in the Khentii Mountains and isolated, sporadic or discontinuous in the western and central parts of the catchment (Sharkhuu 2003). The active layer, which thaws during the short summer, is 1 to 3 m thick, while in coarse material the ground can thaw to depths of 4 to 6 m. The permafrost distribution and its characteristics vary strongly with elevation, aspect, slope, ground material, soil moisture and snow and vegetation cover (Battogtokh et al. 2006).

Main types of land cover within the KRB are grassland, forest and cropland (Tab S2, for a land-use map of the KRB refer to Priess et al. 2014 in the same issue). The Khentii Mountains belong to the mountainous taiga and are mainly covered with needle-leaf forest (MoMo-Consortium 2009). Alpine shrubs and periglacial debris prevail in areas above 2,300 m. In the lower parts, short-grass steppe and arable land predominate. Although the agricultural area makes up only 11 % of the catchment, major parts of the national crop production are carried out in this region. Owing to scarce precipitation, potato and vegetable farming are irrigated. Animal husbandry and crop farming are the dominant land-use activities, followed by open pit mining, which is of high economic importance but of less importance regarding its spatial extend. In the last years, a re-intensification of agriculture is ongoing in the 'Third Campaign of Reclaiming Virgin Lands' by the Mongolian Government (Priess et al. 2011). In addition, an intensification of the mining activities as well as further industrialization and urbanization are expected. The forest area is expected to decrease as a consequence of insufficient reforestation and the threat of forest fires, diseases, clearance and climate change (MoMo-Consortium 2009).

Main water consumption in the KRB is driven by agriculture, domestic, industry and mining, where both groundwater and surface water are used (MoMo-Consortium 2009). Due to limited information especially regarding the amount of water used for irrigation and in industry and mining, the actual amount of total water withdrawal and the corresponding origin can only be estimated with high uncertainty. Currently, neither an effective water distribution system nor regulatory measures are effectively in place.

Data

Long-term observations of river discharge exist for the water gauge Buren Tolgoi, which is located close to the outlet of the KRB into the Orkhon River. For hydrograph analysis and the calibration of the SWAT model, daily discharge rates from Buren Tolgoi for the time period 1991–2002 were used.

Climatic data with varying parameter coverage are available for 12 meteorological stations and 14 posts (the latter have a reduced data availability) (MoMo-Consortium 2009). Daily values for precipitation, temperature, relative humidity, wind speed and solar radiation were interpolated by Wimmer et al. (2009) for the period 1986–2006 on a grid of 1 × 1 km using case-sensitive interpolation and spatial statistical methods. Based on these data, 14 almost uniformly distributed locations for meteorological variables were applied in the SWAT simulations.

The SWAT model was set up using a HydroSHEDS digital elevation model with a resolution of 90 m, developed by the Conservation Science Program of the World Wildlife Fund (WWF) using hydrologically conditioned elevation data of the Shuttle Radar Topography Mission (SRTM) at 3 arc second resolution (Lehner et al. 2006). The river network of the Kharaa River and its tributaries was digitized by colleagues from the Leibniz Institute of Freshwater Ecology and Inland Fisheries (IGB) and the Helmholtz-Center for Environmental Research (UFZ) from LANDSAT satellite images recorded in 2010 and thematic maps in a resolution of 1:200,000. Based on LANDSAT satellite images and river network data, a revised river network was created consisting of river branches that appear to contain the major portion of draining water. Isolated reaches were removed and lines were drawn through reservoirs.

During the first phase of the project 'IWRM-MoMo', a digital soil map of the catchment at a scale of 1:250,000 was compiled (MoMo-Consortium 2009). The map is a refinement of the map 'Soils of Mongolia' (Dorjgotov 2003) improved by data of 26 soil profiles from field sampling in 2008/2009, soil data and reports from Russian–Mongolian soil campaigns and additional information from remote sensing images as well as topographic and thematic maps (Iderjavkhlan 2008). For each of the 28 soil units and sub-units (Tab S1), values of bulk density, organic carbon content, particle distribution, porosity, field capacity and wilting point are available. Missing parameters for the soil parameterization were derived using pedotransfer functions.

Within the project 'IWRM-MoMo', the distribution of land cover was mapped by Priess et al. (2011). For the simulation in SWAT, a gridded land-use map consisting of 1 × 1 km derived from LANDSAT satellite images from 2000 was used (MoMo-Consortium 2009). The conversion of land cover classes to SWAT crop names is shown in Tab S2. The Land Cover/Plant Growth database, which characterizes the SWAT land cover classes, was kept unaltered due to insufficient information on local vegetation properties. Only the maximum leaf area index was reduced for wetlands, agricultural land, wheat and forests taking into account that the vegetation (growth and thus the vegetation) cover in the region is limited due to insufficient rainfall, presence of a short growing season and disturbances such as grazing and wildfires.

Methods

A time series analysis of rainfall runoff events was performed for the years 1991–2002 based on daily measured stream flow and daily precipitation data in order to analyze the intra-annual dynamics of the KRBs hydrology. To characterize the catchment wide storage and the drainage system, autumn base flow recession constants for every

year were calculated for the exponential function proposed by Maillet (1905)

$$Q = Q_0 \times e^{(-\alpha \times t)} \quad (1)$$

where Q is the discharge and Q_0 represents the discharge at the beginning of the recession period, α is the recession constant and t is time in days since the beginning of the recession period. The parameters were estimated using the nonlinear least-squares estimation routine in R (R Development Core Team 2007). The value for α is indicative of the storage capacity of the catchment and the drainage system characteristics. To assess the systematics of stream flow generation in spring, the same constant (here β) was derived for the stream flow rise in spring showing a similar uniformity for different years and likewise appearing as a straight line in the logarithmic representation. Based on the digital filter technique proposed by Arnold et al. (1995), base flow was separated automatically to calculate the base flow recession constant for the shallow groundwater system, which was applied in SWAT.

Two different model setups were prepared in ArcSWAT (SWAT version 2005), one with presence and one with absence of permafrost adaptations. Winter and summer flow paths in the subsurface and the concept of permafrost as modeled within SWAT are shown in Fig. 2. Adaptations were applied directly within the SWAT input settings based on the assumption that the presence of permafrost restricts percolation to deeper groundwater systems due to reduced hydraulic conductivity. Consequently, an impermeable layer was inserted for regions of frozen ground. With this adaption, physical processes in a permafrost environment are reproduced rather than changing real soil dimensions (e.g., the depth of the impermeable layer ensures a reasonable percolation rate but does not necessarily correspond to the exact depth of the active layer). Since permafrost in the region is mainly discontinuous, some percolation was allowed by setting an impermeable layer to a depth of 3.5 m. In SWAT, the difference of 1.5 m from the soil bottom at 2 m to the impermeable layer implies that percolation to the shallow aquifer is restricted to 1 % of the original percolation rate (Eq. 2).

$$\text{perc} = \text{perc}_{\text{orig}} \times \frac{d_{\text{diff}}}{d_{\text{diff}} + \exp[8.833 - 2.598 \times d_{\text{diff}}]} \quad (2)$$

where perc is the water percolating to the shallow aquifer with an impermeable layer (mm), $\text{perc}_{\text{orig}}$ is the water percolating to the shallow aquifer without an impermeable layer (mm) and d_{diff} is the distance from the bottom of the soil profile to the impermeable layer (m). The soil types for permafrost conditions were selected according to the map of permafrost distribution provided by Sharkhuu (2003) (Tab S1).

In winter, also the soil layers freeze, so that water movement in the soil is strongly reduced. SWAT inhibits percolation and lateral flow from soil layers with temperatures below 0 °C. Consequently, SWAT is able to represent the decrease of hydraulic conductivity during winter to some extent. SWAT uses the Natural Resources Conservation Services (previously Soil Conservation Service) curve number (CN) equation to predict surface runoff which implicitly assumes an infiltration excess response to precipitation (Neitsch et al. 2005). When the surface layer of soil is frozen, the generated runoff is increased by modifying CN. Nevertheless, some infiltration occurs if frozen soils are dry.

Precipitation in SWAT is considered as snow according to the mean daily air temperature (Neitsch et al. 2005). Snow cover is modeled using an areal depletion curve. The resulting non-uniform snow cover empirically represents shading, drifting, topography and land cover. Snow melt is a function of the air and snow pack temperatures, the areal coverage of snow and additional calibration factors. The parameters that affect snow fall and snow melt were assigned corresponding to a study of snow sublimation for the KRB (Wimmer et al. 2009). The factor for the lag of snow pack temperature, as well as the minimum snow water content that corresponds to 50 and 100 % snow cover, were adapted during calibration. Snow accumulation and melt were calculated for each sub-basin without further differentiation into elevation bands.

The sub-basins and the stream network were delineated based on the HydroSHEDS DEM using an area of accumulation of 4,500 ha. To improve the allocation of streams especially in areas of strong meandering and in broad river valleys, the revised stream network was superimposed onto the DEM. In total, 187 sub-basins were delineated and used as input for the model. Six land-use categories and 28 soil types were applied to assign hydrological response units (HRUs). Due to the regional context of the study, slope as an additional factor for HRU delineation was not used in order to limit total number of HRUs and computational effort. Overlaying this information, 2,243 sub-units with unique land-use and soil were generated. Applying threshold values for the generation of HRUs as recommended by Winchell et al. (2009), a final number of 706 HRUs was obtained.

The model was run on a daily basis for a period of 11 years (1986–1996), while the last 6 years were used for calibration. As recommended in previous SWAT applications (Neitsch et al. 2004), a warm-up period (5 years) was applied for all model runs. After a calibrated parameter set was found, the model was executed for six additional years (1997–2002) to validate the model. Sensitivity analysis, calibration and validation were performed using discharge data for the outlet of the catchment from the gauge Buren Tolgoi. The calibration of stream flow for the 6-year period

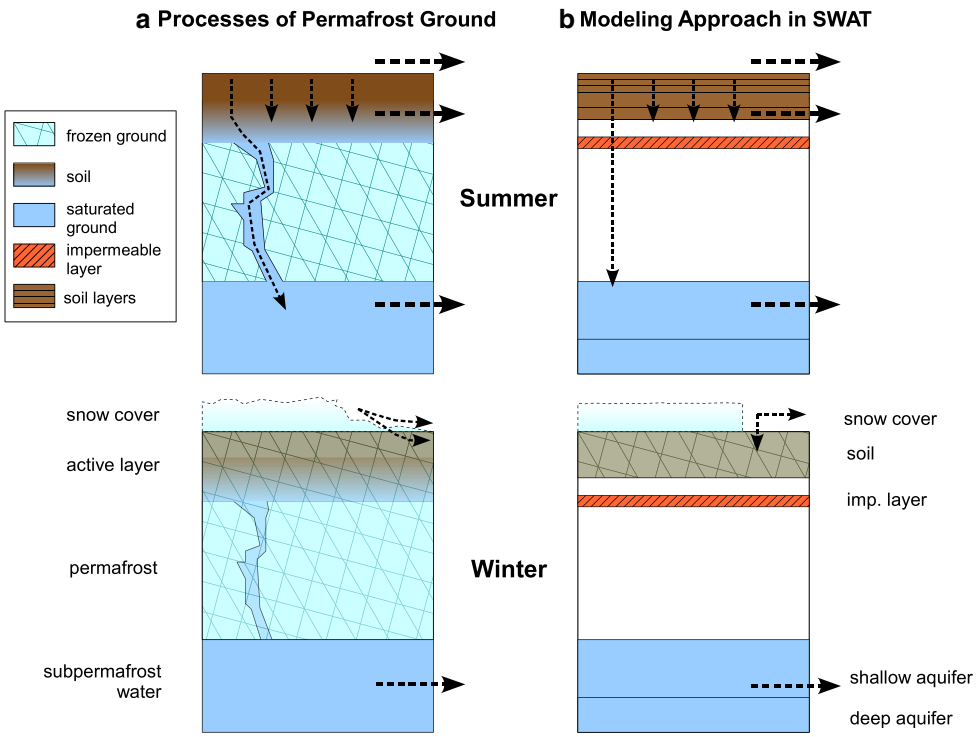

Fig. 2 **a** Water flow paths in discontinuous permafrost soils. **b** Concept of permafrost as modeled with SWAT, including the impermeable layer which was inserted for regions covering frozen ground

was executed manually by fitting the parameters that were identified during sensitivity analysis as well as additional parameters that were assumed to be of high sensitivity although they are not included in the automatic sensitivity analysis. The Nash–Sutcliffe Efficiency (NSE) and the Percent Bias (PBIAS) were used to evaluate the performance of daily and monthly simulation outputs. The NSE is a normalized statistic that states the relative magnitude of the residual variance ('noise') compared to the measured data variance ('information') (Nash and Sutcliffe 1970). It ranges between $-\infty$ and 1, while positive values are generally viewed as acceptable (Moriasi et al. 2007). The Percent Bias (PBIAS) calculates the mean tendency of the simulated data to be larger or smaller than their measured counterparts with 0 being the optimal value (Gupta et al. 1999). Positive values of PBIAS imply model underestimation bias while negative values indicate overestimation. Simulated stream flow was checked for accuracy of fit for different periods considering the discharge producing phenomena. From the SWAT model simulations, the water balance components were quantified.

Results

Stream flow patterns

The discharge of the Kharaa River is characterized by a high intra- and inter-annual variability (Fig. 3). The typical hydrograph of the Kharaa River is dominated by two major runoff periods caused by precipitation events in July and August and snow and ice melt in May. The summer peak is generally more pronounced. In winter, river discharge is strongly dependent on the continuously decreasing base flow component. Although precipitation and hence the total volume of stream flow strongly varies from year to year, the discharge patterns show a large uniformity among the years. Stream flow recession in fall plots as a straight line in the logarithmic representation. The fitted α values range between 0.041 and 0.083 1/d. These correspond to mean hydraulic residence times $t = 1/\alpha$ ranging between 12.1 and 24.3 d. In addition, the rise in spring river discharge could be fitted with the exponential function. Stream flow in spring increases exponentially with similar β values for all years ranging between -0.035 and -0.095 1/d. These β values can be interpreted as an accumulation coefficient that reflects the processes related to snow and ice melt in spring.

SWAT model

Parameters tested during the sensitivity analysis are ranked in Tab S3 with respect to their influence on flow predictions from high to low sensitivity. Parameters which induce more than a 0.1 % change in discharge were considered for optimization. As the base flow alpha factor was derived during a base flow separation procedure (ALPHA_BF = 0.0386), the factor was not altered during calibration. Likewise, the soil

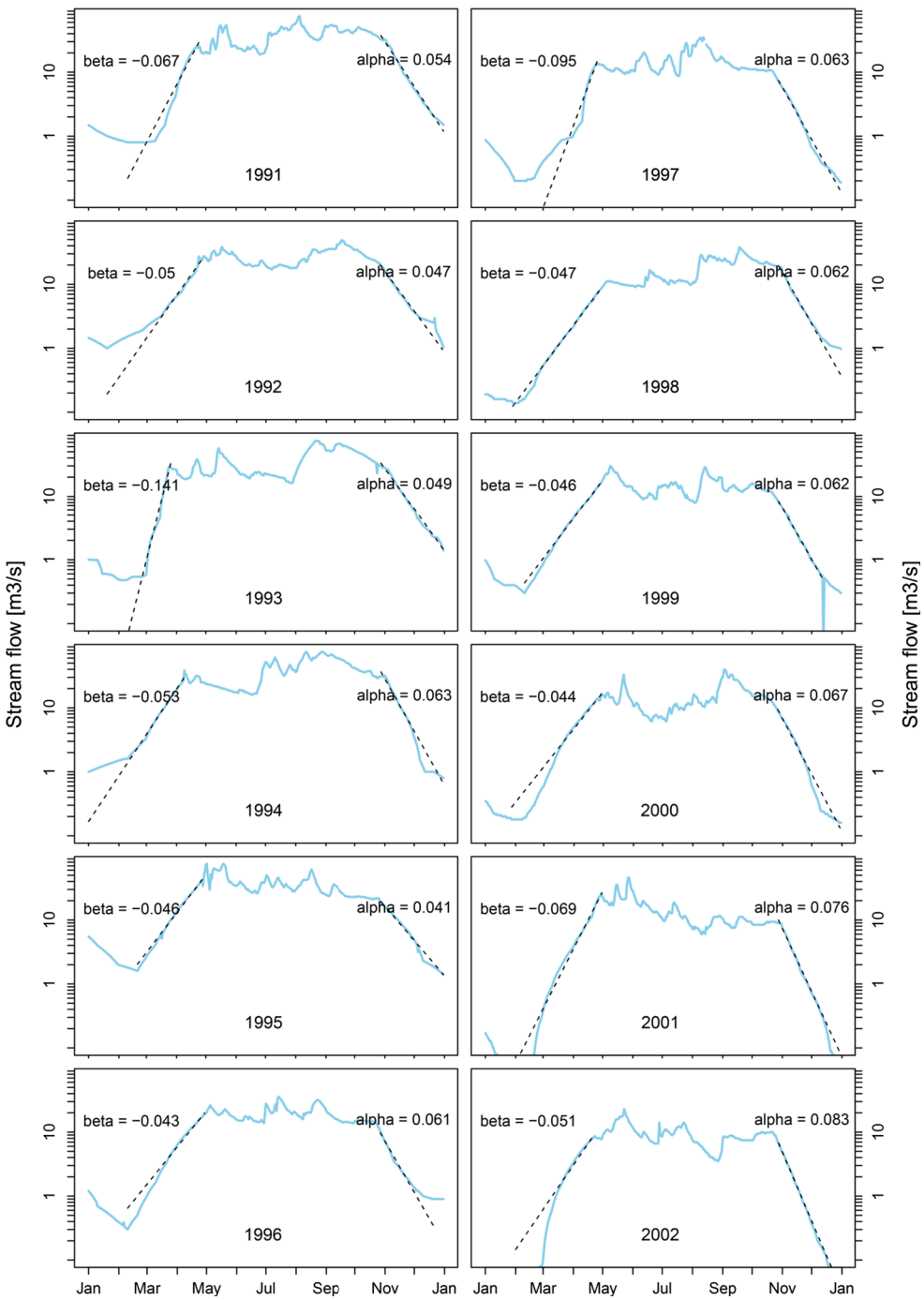

Fig. 3 Fitting of α and β values (1/d) estimated with Eq. 1 for the rising and receding limbs of the annual hydrographs from 1991 to 2002

depth was not included for not modifying the permafrost setting. The calibrated parameter set with the type of adjustments is presented in Tab S4.

The simulated river discharge reflects the two discharge peaks as a response to melt water and precipitation (Fig. 4). By model calibration, simulated stream flow could be improved compared to the uncalibrated model for the years 1991, 1992 and 1995, but summer rainfall peaks are overestimated for the years 1993 and 1994. Calibration of snow parameters allowed an improvement in reproducing spring events, resulting in an increased stream flow in May and June. Regarding the timing, it is obvious that spring runoff starts $\sim$1 month delayed (May instead of April). In case peak discharges are well reflected, the draining of the system is satisfactorily reproduced. Solely in years when summer rainfall events are incorrectly timed or strongly over- or underestimated, base flow recession occurs early or late.

Despite the enhanced model performance, the discrepancy of overestimated peaks in 1993 and 1994 and heavily

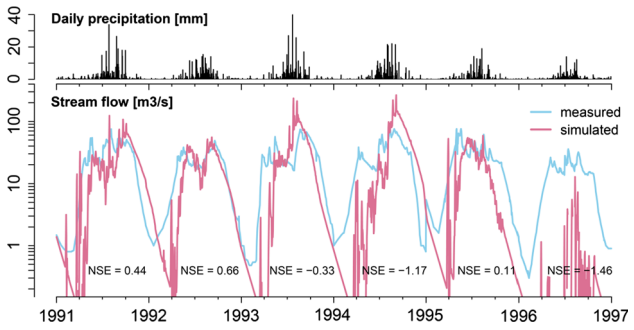

Fig. 4 Daily stream flow (1991–1996): measured and simulated (with permafrost adaptations); NSE is calculated based on monthly averaged values

underestimated stream flow for the entire year in 1996 could not be solved by further model calibration. Consequently, the performance ratings of the calibrated model (Table 1) (NSE = −0.46 for daily and −0.18 for monthly values) are still not fully satisfactory. The PBIAS of 16.11 indicates that the model tends to simulate smaller stream flow than the observed one, although the underestimation is acceptable. For a single year (1992), the calibrated parameter setting resulted in satisfactory (daily) to good (monthly) efficiency statistics (NSE = 0.53 for daily and 0.66 for monthly values).

Simulated stream flow for the validation period 1997–2002 is strongly underestimated (PBIAS = 66.34 for daily and 66.35 for monthly values). Although the model shows a heavy underestimation of stream flow, efficiency statistics (NSE = −0.11 for daily and −0.10 for monthly values) of the validation period are even better than of the calibration period (1991–1996). The main identified problem is that the model completely fails for 1 year but simulates stream flow satisfactorily for the following year. While discharge is underestimated for the entire year 1999, the efficiency statistics for the year 2000 satisfy the demands of Moriasi et al. (2007) (Table 1). No clear trend is recognizable whether the early-year peak or the peak in late summer is simulated with a greater accuracy.

Water balance

The water balance components were quantified based on the simulation period 1991–1996. However, the presented values must be treated with caution due to the mentioned uncertainties regarding the simulation of stream flow patterns. The values shown in Table 1 represent simulated annual values averaged for the entire KRB. Simulated in SWAT, the area receives 319 mm of rain and 32 mm of snow per year on average. Due to high evapotranspiration, 88.3 % of precipitation is lost to the atmosphere. However, only 1 mm sublimates according to SWAT simulations. High evapotranspiration strongly reduces stream flow

Table 1 (a) Average amount of the water balance components based on the simulation period 1991–1996 with presence of permafrost adaptations, (b) annual performance criteria based on monthly outputs

		(mm)	(%) of *P*
Precipitation (*P*)		351	
Snow		32	9.1
Rain		319	90.9
Evapotranspiration		309	88.0
Sublimation		1	0.2
Total stream flow		41	11.7
Surface runoff		2	0.5
Lateral flow		21	5.8
Base flow		19	5.4
Revap		2	0.6
Percolation to shallow aquifer		27	7.6
Recharge to deep aquifer		5	1.5
		NSE	PBIAS
Calibration	1991	0.44	15.37
	1992	0.66	15.53
	1993	−0.33	−1.55
	1994	−1.17	−27.91
	1995	0.11	43.84
	1996	−1.46	97.16
Validation	1997	−0.12	70.76
	1998	−0.46	83.09
	1999	−1.10	88.69
	2000	0.60	31.10
	2001	0.41	47.84
	2002	−0.40	77.72

generation and the contribution to soil and groundwater. The simulated stream flow for the years 1991–1996 accounts for 41 mm on average.

In Fig. 5, the simulated water balance components are presented as average monthly values for the years 1991–1996 comparing (a) absence and (b) presence of permafrost adaptations. Based on this figure, the seasonal variations of the water input components rain and snow as well as of the stream flow components surface runoff, lateral flow and base flow simulated with SWAT can be compared. Furthermore, the generated water yield can be compared with measured stream flow. It is apparent that snow melt as simulated in SWAT contributes considerably to the water input in March and April, while rainfall has increasing importance from May on. However, snow melt does not instantaneously result in an increased stream flow but causes higher lateral flow in May and higher base flow in June. While surface runoff is the fastest stream flow component, lateral flow occurs delayed followed by even slower base flow contribution. Modeled lateral flow and

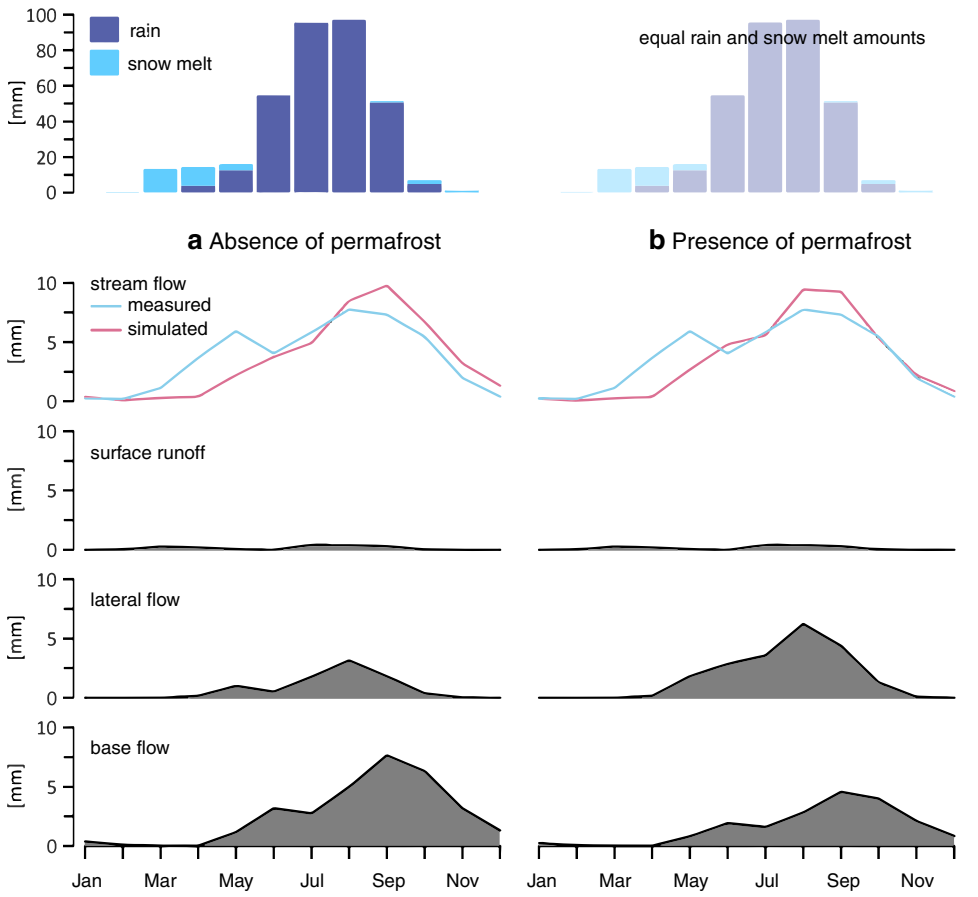

Fig. 5 Mean monthly water balance components based on SWAT outputs compared with measured stream flow (1991–1996): **a** with absence of permafrost, **b** with presence of permafrost. Note: rainfall and snow melt are identical for both settings

base flow are affected by the permafrost setting. As the impermeable layer favors lateral flow, the hydrograph is shifted slightly forward. The generated water yield with the permafrost setting therefore shows small improvements concerning simulated stream flow in May and June.

Discussion

Hydrological regime

In spite of highly variable annual precipitation, the hydrograph of the Kharaa River shows striking patterns indicating systematic and annually recurring processes that dominate the seasonal distribution of stream flow. Similar β values and a similar timing of stream flow rise in spring suggest that the observed pattern results from the process of thawing, which is induced by the increase of temperature above 0 °C. Thawing concerns all water storages that freeze during winter, in particular snow cover, water in the soil and the subsurface and water stored in icings (Sloan and Van Everdingen 1988; Woo et al. 2000). Wimmer et al. (2009) found that snow covers in the KRB are heavily reduced by high sublimation rates of ~80 % of total snow fall. Therefore, the melt of snow covers cannot result in the entire stream flow during spring. Hence, the remaining part must be formed by soil and subsurface water as well as by the melting of aufeis. However, these sublimation rates could not be replicated by the SWAT model since the modeling approach does not account for the formation and melt of river ice. Consequently, snow related parameters had to be calibrated to compensate for all melting processes and to ensure a sufficient amount of simulated river discharge in spring but lose their physical meaning. In discontinuous permafrost regions similar to the KRB, icings were found to represent up to 30 % of annual groundwater discharge, strongly contributing to spring discharge (Woo et al. 2000). Froehlich and Slupik (1982) described the melting process of icings in the Khangai Mountains in Mongolia, where aufeis is even more extensive. With increasing air temperature, ice covers start to melt beginning at large springs and where groundwater discharges to the river channel. As melting progresses, the discharge rate gradually increases. This is consistent with the exponential increase of observed stream flow. Once snow and ice have melted in May, river discharge decreases.

With the beginning of precipitation in June and July, stream flow of the Kharaa River rises instantly. The shape of the summer hydrograph depends strongly on precipitation

events and is consequently more variable. Strong rainfall in summer contributes less to direct flow but more to the groundwater flow component than the melt of snow covers because the infiltration and water holding capacity of the soils is increased when the active layer thaws (Bolton 2006). In summertime, the water storages in the subsurface are filled. From October on, when temperature drops below 0 °C, rainfall occurs as snow. Together with lower precipitation, this results in the depletion of groundwater and soil storages and in the exponential decrease in stream flow in fall and winter. Hence, the base flow component becomes more important towards the end of the year. Due to decreasing temperatures and proceeding of aufeis formations, recorded base flow is smaller than the actual groundwater contribution. Consequently, stream flow decreases faster than without the formation of aufeis and derived α values are larger. Therefore, α values under subarctic conditions depend not only on the drainage system and the catchment wide storage but also on the characteristics of aufeis formation.

SWAT model

Runoff in the KRB is exceedingly low so that generally, the application of hydrological models is crucially impeded. The simulation of stream flow using the SWAT model faces certain difficulties that are related to the particular climatic conditions. Simulations could satisfactorily reflect discharge for single years but were not reliable for a longer time period. This is consistent with a previous study that found SWAT to perform better under wet conditions when the model was calibrated with highly variable meteorological data from a mix of wet and dry years (Rahbeh et al. 2011). The model performed well for the simulation of runoff from precipitation and for base flow recession. Stream flow as a response to snow and ice melt could be improved during calibration but was still underestimated.

Due to the insufficient representation of processes with high hydrological relevance for subarctic conditions (e.g. aufeis, sublimation) in SWAT, single model parameters could not be satisfactorily calibrated with a physical meaning. Despite this fact, the simulated water balance components meet the magnitudes from earlier studies. Evapotranspiration losses are in accordance with evapotranspiration ranging from 80 to 90 % as stated by Menzel et al. (2011) for the period 1990–2002 and by Ma et al. (2003) quantifying evapotranspiration at 86 % of precipitation for the years 1988–1992. For the groundwater-bearing area of the Selenga Catchment, groundwater recharge was estimated as 20 mm/year (=5.40 × 109 m^3/year) (Mun et al. 2008). In the presence of permafrost, a similar amount of percolation to the aquifers of 27 mm/year could be simulated with SWAT. For all estimates considering water resources special caution is required, since the model performance is still not sufficient for detailed recommendations. However, the general magnitudes are met.

Stream flow in response to snow melt is underestimated in SWAT since most of the generated snow melt is simulated to infiltrate and does not directly contribute to river discharge but increases the soil water content or contributes to groundwater recharge. However, overland flow on impermeable frozen ground is common for permafrost regions since melt water is hampered to infiltrate (Woo and Winter 1993). The difficulty of modeling varying infiltration behavior for spring and summer is already documented (Niu and Yang 2006). Using the HBV model, Sand and Kane (1986) observed a relative underestimation of snow melt runoff and overestimation of rainfall runoff. They included the influence of the active layer by using one set of soil parameters for the snow melt period and a second set for the rainfall period in summer.

Although soils are allowed to freeze in SWAT, no deeper penetration of frost into the ground, necessary to reflect permafrost (e.g. freezing of the shallow aquifer), is described by the current version of SWAT. Frozen ground results in a strong decrease in hydraulic conductivity down to nearly impermeable layers. Consequently, permafrost acts like a barrier for the flow of groundwater and restricts groundwater recharge and discharge to unfrozen areas (Williams 1970). This effect of permafrost was reproduced by assigning an impermeable layer in the subsurface to the areas dominated by permafrost. The simulations indicated that this parameterization was suitable to prevent aquifer recharge in permafrost areas and alter the composition of stream flow towards more lateral and less groundwater flow, which can be a suitable interim solution to better reflect hydrological processes characterizing permafrost areas. However, this setting has not shown a considerable effect on a more pronounced response of snow melt. The settings to represent permafrost presence and the influence of the active layer need to be aligned simultaneously to capture the seasonally varying infiltration behavior. Although in general recommended for humid conditions, the SWAT-VSA (VSA = various source areas) model (Easton et al. 2008) could be applied to the KRB. This modification of the original SWAT model allows for the generation of storm runoff by saturation excess on various source areas and improves runoff simulation for permeable soils underlain by a shallow restricting layer similar to permafrost.

SWAT is currently not able to simulate the formation and melt of river icings, which were identified to be important for the generation of stream flow during spring as well as for base flow recession in fall. However, the latter could be reflected by the model, the base flow recession coefficient applied in SWAT characterizes not

only the processes of aquifer drainage but also the formation of river icings. The coupled model by Ma and Fukushima (2002), which includes the formation of river ice using accumulated degree-days, improved the performance of stream flow predictions. Coupling a similar model with SWAT or including the process in the model itself could enhance both draining during winter and stream flow increase in spring. An approach that considers the amount of base flow for the formation of icings in each sub-basin would be favorable.

The difficulties involved in estimating the water amounts are strongly related to data quality, model setup and the parameterizations that define precipitation inputs and losses to the atmosphere and to deep drainage. In particular, discharge measurements in cold areas are vulnerable to uncertainty since stage–discharge relationships are altered due to river ice (Lévesque et al. 2008). The input data cannot cover all variability but did not restrict the applicability of SWAT to the investigated area. However, better spatial and temporal resolution of the data can strongly improve the model calibration.

Conclusion

The KRB combines several challenges for hydrological studies. On the one hand, the overall spatial and temporal variabilities are high. On the other hand, water availability is strongly reduced due to large evapotranspiration rates. At the same time, low temperatures complicate flow patterns due to freezing in the subsurface and give rise to snow and river icings.

The development of modeling tools, such as SWAT, is required for the implementation of IWRM strategies. Analysis of the hydrograph and applying SWAT to the KRB could provide valuable support in identifying and localizing important processes, namely surface runoff and infiltration in presence of frozen ground and river ice formation and melt, driving the regional hydrology and improving the description of hydrological processes in model approaches. The uncertainties included in the quantification of the water balance components could be reduced by the calibration and modification of SWAT; however, there is still need for improved data input, model parameterization and process representation. Especially, refinements are necessary regarding a seasonally varying infiltration behavior and the incorporation of river ice formation and melt. Special caution is required for assigning parameters of evapotranspiration and snow cover which trigger uncertainty in the simulations.

Based on the current state of the model and the recommendations that have been formulated, the SWAT model should be further developed in order to be applicable and transferable to different and critical hydrological conditions and regimes. A more precise quantification of individual water balance components would largely reduce the uncertainty with respect to the identification of IWRM measures. Findings of this study concerning the hydrological processes in the KRB are expected to be beneficial for future modeling intentions and for the implementation of an IWRM. In particular, the insights into the subarctic processes enhance the understanding of important hydrological conditions in the catchment and highlight the demand of considering the complexity of subarctic phenomena in further studies.

Acknowledgments The results presented in this paper are based on the research and development project ‘Integrated Water Resources Management in Central Asia: Model Region Mongolia’, funded by the German Federal Ministry of Education and Research (BMBF) in the framework of the FONA (Research for Sustainable Development) initiative (Grant No. 033L003). We acknowledge the support provided by the Project Administration Jülich (PTJ) and the BMBF/International Bureau in the context of the ‘Assistance for Implementation’ (AIM) scheme. The authors also like to thank the German Academic Exchange Service (DAAD) that gave financial support in form of a PROMOS scholarship for a research stay in Mongolia. We also gratefully acknowledge the critical comments by two anonymous reviewers.

References

Arnold JG, Allen PM, Muttiah R, Bernhardt G (1995) Automated base flow separation and recession analysis techniques. Ground Water 33(6):1010–1018. doi:10.1111/j.1745-6584.1995.tb00046.x

Arnold JG, Srinivasan R, Muttiah RS, Williams JR (1998) Large area hydrologic modeling and assessment—part I: model development. J Am Water Resour Assoc 34(1):73–89

Batima P, Tatsagdorj L, Gombluudev P, Erdenetsetseg B (2005) Observed climate change in Mongolia, AIACC Working Paper No. 12, Assessments of Impacts and Adaptations to Climate Change (AIACC)

Batimaa P, Myagmarjav B, Batnasan N, Jadambaa N, Khishigsuren P (2011) Urban water vulnerability to climate change in Mongolia. Ministry of Nature, Environment and Tourism, Government of Mongolia

Battogtokh D, Jambaljav Y, Dashtseren A, Sharkhuu N, Ishikawa M, Zhang Y, Iojima Y, Kadota T, Ohata T (2006) Features and mapping of permafrost distribution in Ulaabaatar area, Mongolia. In: International workshop on terrestrial change in Mongolia—joint workshop of IORGC, MAVEX, RAISE and Other Projects, Tokyo, Japan

Beckers J, Smerdon B, Wilson M (2009) Review of hydrological models for forest management and climate change applications in British Columbia and Alberta. FORREX Forum for Research and Extension in Natural Resources Society, Kamloops

Bolton WR (2006) Dynamic modeling of the hydrological processes in areas of discontinuous permafrost. Dissertation, University of Alaska, Fairbanks

Dorjgotov D (2003) Soils of Mongolia, Ulaanbaatar

Easton ZM, Fuka DR, Walter MT, Cowan DM, Schneiderman EM, Steenhuis TS (2008) Re-conceptualizing the soil and water assessment tool (SWAT) model to predict runoff from variable

source areas. J Hydrol 348(3–4):279–291. doi:10.1016/j.jhydrol.2007.10.008
Froehlich W, Slupik J (1982) River icings and fluvial activity in extreme continental climate, Khangai Mountains, Mongolia. In: French HM (ed) National Research Council of Canada, Associate Committee on Geotechnical Research, pp 203−211
Grayson R (2010) Asian ice shields and climate change. World Placer J 10:21–45
Gupta HV, Sorooshian S, Yapo PO (1999) Status of automatic calibration for hydrologic models: comparison with multilevel expert calibration. J Hydrol Eng 4(2):135–143. doi:10.1061/(Asce)1084-0699(1999)4:2(135
Hofmann J, Venohr M, Behrendt H, Opitz D (2010) Integrated water resources management in central Asia: nutrient and heavy metal emissions and their relevance for the Kharaa River Basin, Mongolia. Water Sci Technol 62(2):353–363. doi:10.2166/wst.2010.262
Hofmann JM, Watson V, Scharaw B (2014) Groundwater quality under stress: contaminants in the Kharaa River Basin (Mongolia). Environ Earth Sci (this issue). doi:10.1007/s12665-014-3148-2
Hu XG, Pollard WH (1997) The hydrologic analysis and modelling of river icing growth, North Fork Pass, Yukon Territory, Canada. Permafr Periglac Process 8(3):279–294. doi:10.1002/(Sici)1099-1530(199709)8:3<279:Aid-Ppp260>3.0.Co;2-7
Iderjavkhlan S (2008) Digital soil map of the Kharaa River Basin—report. Institute of Geography, Mongolian Academy of Sciences; IWRM-MoMo, CESR, University of Kassel
Karthe D, Malsy M, Kopp S, Minderlein S, Hülsmann L (2013) Assessing water availability and its drivers in the context of an integrated water resources management (IWRM): a case study from the Kharaa River Basin, Mongolia. Geo-Öko 34(1–2):5–26
Karthe D, Heldt S, Houdret A, Borchardt D (2014) Development and implementation of a science-based IWRM in a country under rapid transition: lessons learnt from the Kharaa River Basin, Mongolia. Environ Earth Sci (this issue). doi:10.1007/s12665-014-3435-y
Lehner B, Verdin K, Jarvis A (2006) HydroSHEDS technical documentation version 1.0
Lévesque É, Anctil F, Van Griensven A, Beauchamp N (2008) Evaluation of streamflow simulation by SWAT model for two small watersheds under snowmelt and rainfall. Hydrol Sci J 53(5):961–976
Ma XY, Fukushima Y (2002) A numerical model of the river freezing process and its application to the Lena River. Hydrol Process 16(11):2131–2140. doi:10.1002/Hyp.1146
Ma X, Yasunari T, Ohata T, Natsagdorj L, Davaa G, Oyunbaatar D (2003) Hydrological regime analysis of the Selenge River Basin, Mongolia. Hydrol Process 17(14):2929–2945
Maillet E (1905) Essais d'hydraulique souterraine et fluviale. Libraire Sci, A Herman, Paris (Cited by Hall (1968))
Menzel L, Hofmann J, Ibisch R (2011) Untersuchung von Wasser- und Stoffflüssen als Grundlage für ein Integriertes Wasserressourcen-Management im Kharaa-Einzugsgebiet, Mongolei. Hydrologie und Wasserbewirtschaftung 55(2):88–103
MoMo-Consortium (2009) Integrated water resources management for Central Asia—model region Mongolia (MoMo): case study in the Kharaa River Basin. Final Project Report
Moriasi DN, Arnold JG, Liew MWV, Bingner RL, Harmel RD, Veith TL (2007) Model evaluation guidelines for systematic quantification of accuracy in watersheds simulations. Trans ASABE 50(3):885–900. doi:10.13031/2013.23153
Mun Y, Ko IH, Janchivdorj L, Gomboev B, Kang SI, Lee C (2008) Integrated water management model on the Selenge River Basin Status Survey and Investigation (Phase I). Korea Environment Institute, Seoul
Nash JE, Sutcliffe JV (1970) River flow forecasting through conceptual models part I—a discussion of principles. J Hydrol 10(3):282–290
Neitsch SL, Arnold JG, Kiniry JR, Srinivasan R, Williams JR (2004) Soil and water assessment tool—Input/Output File Documentation. Temple, Texas
Neitsch SL, Arnold JG, Kiniry JR, Williams JR (2005) Soil and water assessment tool—Theoretical Documentation. Temple, Texas
Niu GY, Yang ZL (2006) Effects of frozen soil on snowmelt runoff and soil water storage at a continental scale. J Hydrometeorol 7(5):937–952. doi:10.1175/Jhm538.1
Priess JA, Schweitzer C, Wimmer F, Batkhishig O, Mimler M (2011) The consequences of land-use change and water demands in Central Mongolia. Land Use Policy 28(1):4–10. doi:10.1016/j.landusepol.2010.03.002
Priess J, Schweitzer C, Batkhishig O, Wurbs D, Koschitzki T (2014) Impacts of land-use dynamics on erosion risk and water management in Northern Mongolia. Environ Earth Sci (this issue). doi:10.1007/s12665-014-3380-9
R Development Core Team (2007) R: a language and environment for statistical computing. R Foundation for Statistical Computing, Vienna
Rahbeh M, Chanasyk D, Miller J (2011) Two-way calibration–validation of SWAT model for a small prairie watershed with short observed record. Can Water Resour J 36(3):247–270. doi:10.4296/cwrj3603884
Sand K, Kane DL (1986) Effects of seasonally frozen ground on snowmelt modeling. In: Kane DL (ed) Proceedings of the symposium: cold regions hydrology. American Water Resources Association, pp 321–327
Sharkhuu N (2003) Recent changes in the permafrost of Mongolia. In: Phillips M, Springman SM, Arenson LU (eds) Permafrost. Swets & Zeitlinger, Lisse, pp 1029–1034
Sloan CE, Van Everdingen RO (1988) Region 28, Permafrost region. In: Back W, Rosenshein JS, Seaber PR (eds) The geology of North America, Vol O-2, Hydrogeology. The Geological Society of America, Boulder, pp 263–270
Williams JR (1970) Ground water in the permafrost regions of Alaska. Geological Survey Professional Paper. United States Government Printing Office, Washington
Wimmer F, Schlaffer S, Aus Der Beek T, Menzel L (2009) Distributed modelling of climate change impacts on snow sublimation in Northern Mongolia. Adv Geosci 21:117–124
Winchell M, Srinivasan R, Luzio MD, Arnold J (2009) ARCSWAT 2.3.4 interface for SWAT2005—User's Guide. Temple, Texas
Woo MK, Winter TC (1993) The role of permafrost and seasonal frost in the hydrology of northern wetlands in North-America. J Hydrol 141(1–4):5–31. doi:10.1016/0022-1694(93)90043-9
Woo MK, Marsh P, Pomeroy JW (2000) Snow, frozen soils and permafrost hydrology in Canada, 1995–1998. Hydrol Process 14(9):1591–1611. doi:10.1002/1099-1085(20000630)14:9<1591:Aid-Hyp78>3.0.Co;2-W